Understanding anthracycline action: molecular insights to improve cancer therapy

Gelder, M.A. van

CHAPTER 5

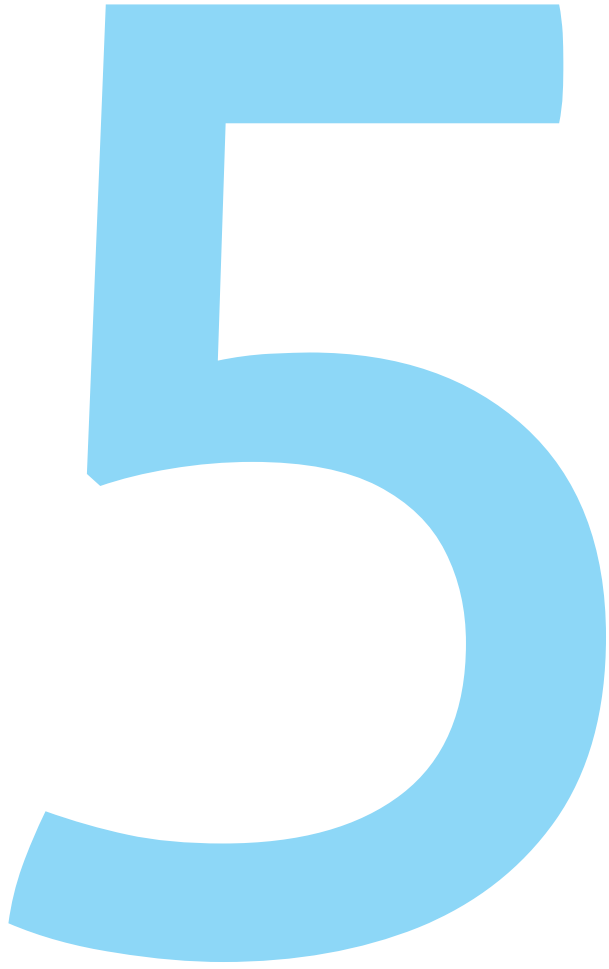

Conclusion and Future Prospects

Anthracyclines are potent chemotherapeutics used to treat various cancers, such as leukemias, lymphomas, and solid tumors. They are characterized by their tetracyclic structure, which facilitates DNA intercalation, connected to an amino sugar that can interact with the DNA backbone phosphodiesters through salt bridges.[1] This intrinsic capacity underlies two main modes of anthracycline action: the generation of DNA double stranded breaks (DNA damage) and eviction of histones from chromatin (chromatin damage).[2] Despite their effectiveness, anthracycline treatment is associated with severe side effects, including long-term issues such as cardiotoxicity, gonadotoxicity and secondary tumorigenesis.[3] These side effects are particularly concerning due to their significant impact on the quality of life of cancer patients. Previous research has suggested that the DNA-damaging function of anthracyclines is primarily linked to these side effects, indicating that anthracyclines that only cause chromatin damage might be preferable over standard therapy.

In **chapter 2**, we evaluated a total of 26 anthracycline variants for their cytotoxicity, DNA damage and chromatin damage activities, making it one of the largest structure-activity relationship study of anthracyclines to date. From this study, we derived several general guidelines regarding the potency and modes of action of anthracyclines. These are: (1) The main cytotoxic activity of the compounds is associated with histone eviction rather than DNA double strand break induction; (2) Generally, *N,N*-dimethylation eliminates DNA double strand break formation without compromising cytotoxicity; (3) Small modifications in the tetracyclic aglycone further contribute to cytotoxicity, as illustrated by the differences in cytotoxicity between doxorubicin and idarubicin; (4) The position of the amine on the sugar moiety has minor effects; and (5) Replacing the amine by an OH or H group significantly reduces cytotoxicity.

The importance of distinguishing between different modes of anthracycline action has been demonstrated by previous studies, which showed that the combination of DNA damage and histone eviction—as exhibited by doxorubicin—results in the major side effects associated with this drug.[4] Anthracyclines that solely induce chromatin damage, such as aclarubicin and *N,N*-dimethyldoxorubicin, are at least as effective against tumor cells as doxorubicin but are less toxic to healthy cells and tissues. For instance, *N,N*-dimethyldoxorubicin does not cause cardiotoxicity, secondary tumor formation, or gonadal dysfunction in murine *in vivo* models.[4] Furthermore, clinical observations indicate that aclarubicin treatment is less cardiotoxic for cancer patients than doxorubicin treatment, while both compounds appear equally effective as anticancer agents.[5,6] These results suggest that separating DNA damage from chromatin damage activities may guide the development of novel variants that lack the major long-term side effects that are associated with currently used anthracycline variants.

Although *N,N*-dimethyldoxorubicin was proven less cardiotoxic in *in vivo* murine models, this has not yet been established in patients. Given the thousands of research papers suggesting that impaired mitochondrial function is associated with cardiotoxicity, we selected six compounds from **chapter 2,** including *N-N*-dimethyldoxorubicin, to investigate their effects on mitochondrial function.

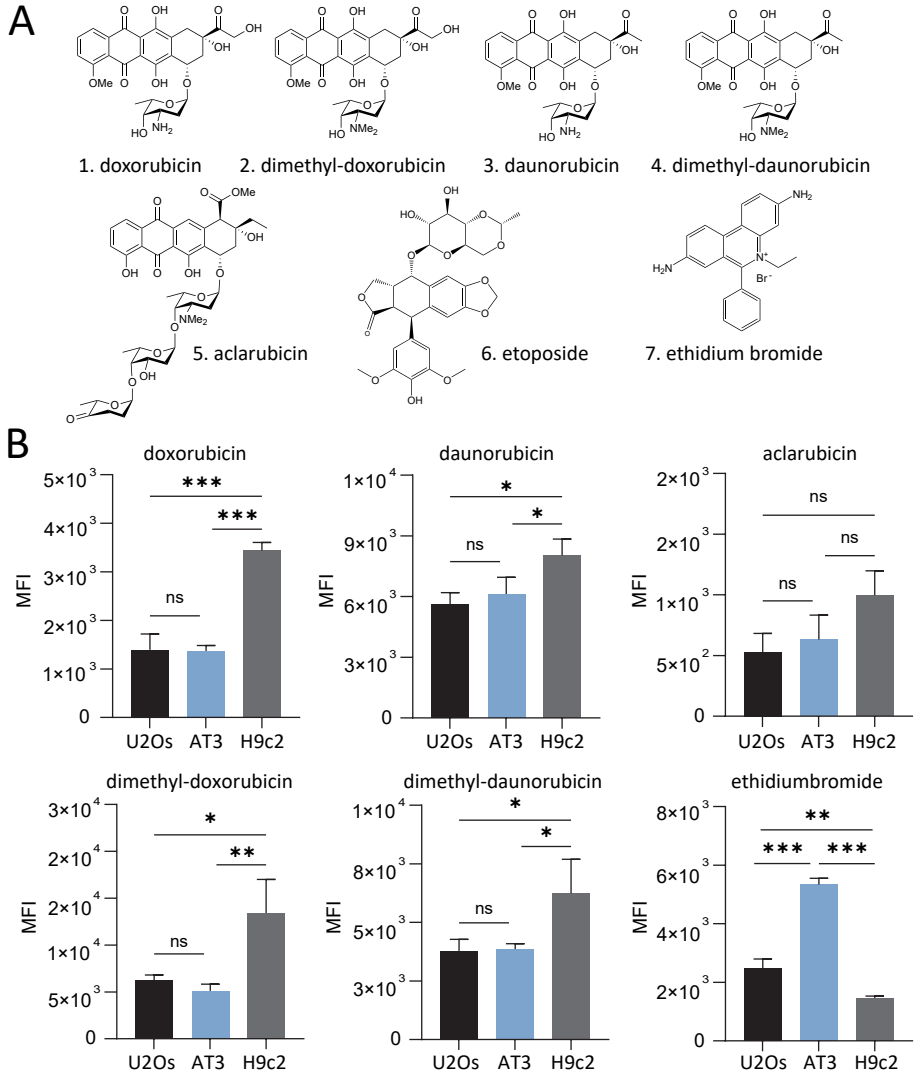

Figure 1 – Chemical structures of anthracycline variants and their cellular uptake. (A) Chemical structures of different anthracycline variants, etoposide, and ethidium bromide. (B) Cellular uptake after 2 hours incubation with different compounds. Intracellular accumulation was measured with flow-cytometry, and mean fluorescent intensity is plotted for all compounds. Ordinary one-way ANOVA, * $p < 0,05$; ** $p < 0,01$; *** $p < 0.001$.

Of these variants, doxorubicin (**1**) and daunorubicin (**3**) induce both DNA and chromatin damage, while *N,N*-dimethyldoxorubicin (**2**), *N,N*-dimethyldaunorubicin (**4**) and aclarubicin (**5**) induce only chromatin damage. Etoposide (**6**) was included as a control that induces only DNA damage, and ethidium bromide (**7**) served as a control for DNA intercalation. (Figure 1A).

We conducted initial experiments as part of a structure-activity relationship study focusing on mitochondrial function. First, we compared the cellular uptake of these anthracyclines and ethidium bromide in two cancer cell lines (U2Os and HeLa) and a myoblast derived cardiac cell line (H9c2). Interestingly, the uptake of all anthracyclines was increased in H9c2 cells compared to both cancer cell lines, although this was not the case for ethidium bromide (Figure 1B). This finding aligns with previous research suggesting that heart tissue is a preferential site for anthracycline accumulation. The most significant effect was observed for doxorubicin, which showed a two-fold higher cellular uptake in cardiac cells compared to the cancer cell lines used. The cell type specific uptake of anthracyclines may be related to the expression of import transporters. Several members of the solute carrier (SLC) superfamily of membrane transporters have been linked to cell-type specific toxicity profiles in response to anthracyclines.[7] However, comparing the cytotoxicity of these compounds in cardiac H9c2 cells to that in U2Os and AT3 cancer cells revealed that all selected compounds, including doxorubicin, were significantly less cytotoxic in H9c2 cells despite the increased uptake (data not shown). This may be due to the higher proliferation rates of both cancer cell lines compared to the cardiac cells. Our data indicate that cellular uptake of anthracyclines is not directly linked to cytotoxicity in the cell lines used in this study, but future research could address whether the expression of SLC importers are regulating cell-type specific accumulation and toxicities of anthracyclines.

In terms of molecular mechanism, we explored whether there is overlap between the effects observed in the nucleus and those in the mitochondria. We confirmed the DNA damaging activity of the selected compounds in the nucleus and aimed to assess the damage to mitochondrial DNA too. Doxorubicin and daunorubicin caused DNA double stranded breaks in genomic DNA (Figure 2A), but we could not detect any mitochondrial DNA damage (Figure 2B). High concentrations of hydrogen peroxide did induce damage of mitochondrial DNA, as expected based on previous reports.[8] In contrast to previous reported literature[9], we could not detect any lesions caused by doxorubicin using the long-range PCR method. Earlier research has indicated a depletion of mtDNA in response to anthracyclines[10], which may contribute to this discrepancy, as our protocol controls for total mtDNA levels. Although the long-range PCR method is frequently used, it has some major limitations. First, DNA lesions that do not significantly stall progression of DNA polymerases will not be detected. Compounds that cause oxidative stress, such as

H_2O_2, are thought to produce more than one type of lesion[11] and anthracyclines may act similarly. The nature of specific lesions cannot be detected with PCR-based methods, but this limitation is shared by other methods available.[12] In addition, the method is based on the expectancy that for most DNA damaging agents, lesions will be introduced randomly in both genomic DNA and mitochondrial DNA. In the case of anthracyclines, this assumption may be incorrect, based on observations of preferential sites of DNA double stranded breaks induction in genomic DNA.[13]

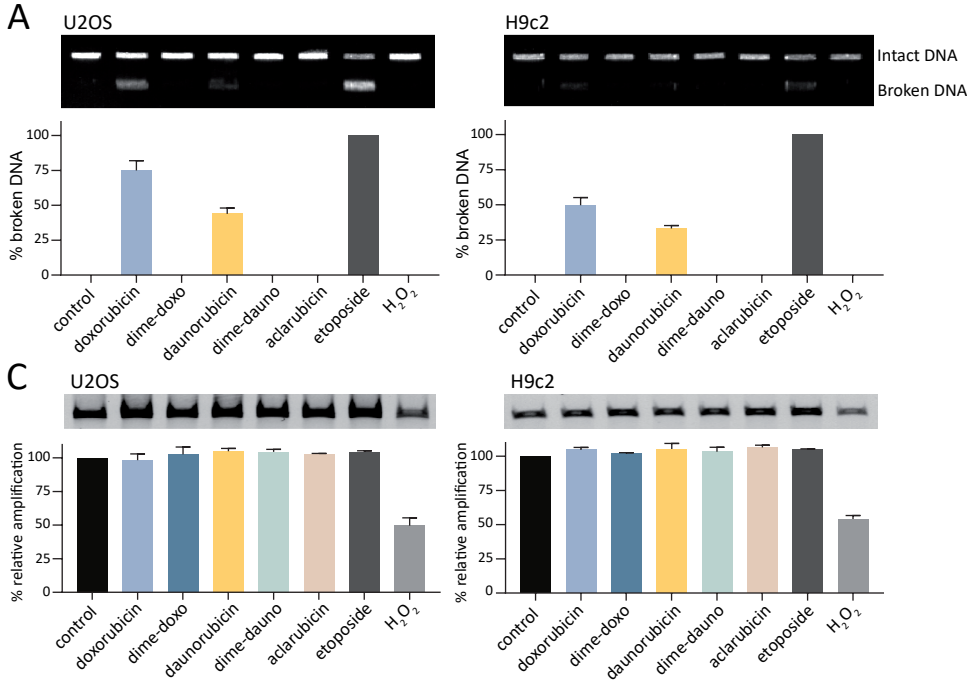

Figure 2 – Nuclear and mitochondrial DNA damage induced by anthracyclines. (A) Nuclear DNA double strand breaks were directly visualized by CFGE in U2OS cells and H9c2 cells. The position of intact and broken DNA is indicated, broken DNA was quantified relative to total DNA. (B) Mitochondrial DNA damage was assessed using long-range PCR in U2OS cells and H9c2 cells. DNA amplification was quantified relative to untreated control cells.

Due to the circular nature of mtDNA (16.6 kb)[14] we validated whether these anthracyclines intercalate into circular plasmid DNA of similar size and examined any differences between anthracycline variants in terms of intercalation. The intercalation of anthracyclines was tested using a competition dye displacement assay with ethidium bromide (Figure 3A) and PicoGreen (Figure 3B). These dyes were chosen because of their

fluorescence upon binding to double-stranded DNA and the addition of compounds that displace the dye results in a loss of fluorescence signal. Plotting the remaining fluorescence against compound concentrations (Figure 3B) revealed that doxorubicin has the highest DNA binding affinity, followed by *N,N*-dimethyldoxorubicin, which was only slightly less efficient. Daunorubicin and *N,N*-dimethyldaunorubicin demonstrated equal DNA intercalation efficiency. The non-intercalating Topo II inhibitor etoposide was used as a negative control. From these results we can deduct that these anthracycline variants could all intercalate into circular, and thus likely also mitochondrial DNA. However, we cannot fully account for the degree in which these anthracycline variants accumulate in the mitochondria to start with. We performed a pilot experiment that confirmed accumulation of doxorubicin, *N,N*-dimethyldoxorubicin, daunorubicin and *N,N*-dimethyldaunorubicin in the mitochondria (data not shown). There are numerous reports about doxorubicin and daunorubicin entering and accumulating in mitochondria[15], but it remains a challenge to compare different anthracycline variants with flow-cytometry or microscopy because of their different fluorescence properties.

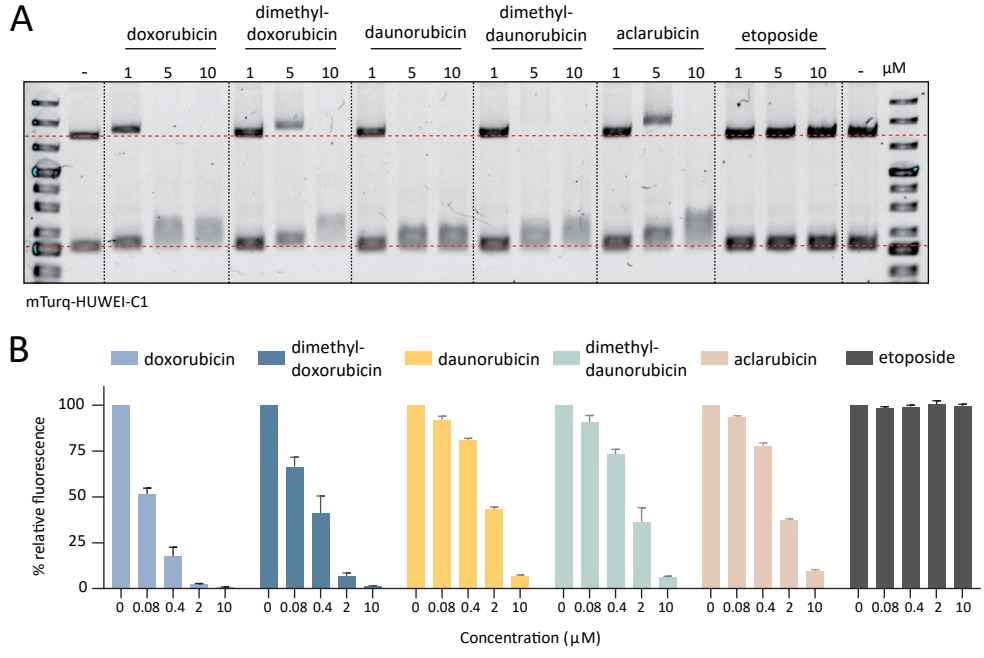

Figure 3 – DNA intercalation affinity of anthracycline variants. (A) The intercalation of anthracyclines into circular double-stranded DNA was tested in a competition dye displacement assay with ethidium bromide. (B) Intercalation affinity was quantified with PicoGreen. The percentage of initial fluorescence is plotted against the concentrations of the indicated compounds.

Previous research has shown that anthracyclines can alter genomic DNA transcription, and that the effects are region-specific for different anthracyclines.[16] We aimed to validate if mitochondrial DNA transcription is similarly altered in response to anthracycline treatment. To this end, we selected genes from three different regions of the circular mitochondrial DNA: mt-ND1, mt-CYB, and mt-CO1. These genes encode proteins that are part of the mitochondrial respiratory chain: NADH dehydrogenase 1, cytochrome b, and cytochrome c oxidase I, respectively.

In both cell lines tested, we observed a trend towards decreased expression of mt-ND1 and mt-CYB in response to anthracycline treatment, while the effects on mt-CO1 expression were less pronounced (Figure 4). Treatment with etoposide or hydrogen peroxide did not alter the expression of mt-ND1, mt-CYB, or mt-CO1, supporting the hypothesis that DNA intercalation is important for the disruption of gene expression. Region-specific DNA intercalation may also contribute to the observed differences between anthracyclines.

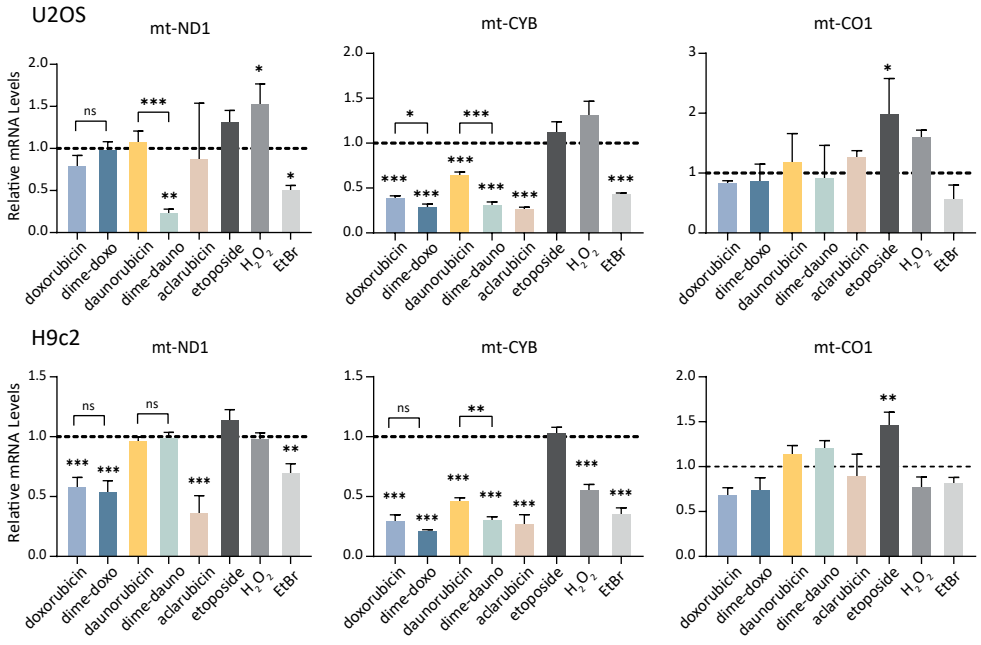

Figure 4 – The effect of anthracycline variants on the expression of mitochondrial genes. The expression of mRNA levels of mt-ND1, mt-CYB and mt-CO1 was measured with RT-QPCR in U2OS cells and H9c2 cells 4 hours post anthracycline treatment. Ordinary one-way ANOVA with Dunnett's multiple comparison test, * $p < 0,05$; ** $p < 0,01$; *** $p < 0.001$.

The location of mt-CYB near the D-loop and origin of replication for the mitochondrial heavy strand – sites serving as central hubs for mtDNA replication and transcription[17] – could explain why the expression of this gene is particularly affected compared to mt-ND1 and mt-CO1. Regiospecificity has been described for different anthracycline variants in the context of genomic DNA. For instance, doxorubicin specifically induces double-stranded breaks near active promoter regions[13], and the intercalation of daunorubicin is partially dependent on GC content.[18] This regiospecificity extends to different chromatin states, with doxorubicin and daunorubicin preferentially binding to open chromatin regions, while aclarubicin also intercalates into condensed chromatin.[16] Future research employing a ChIP-seq-like protocol specifically designed for mitochondrial DNA may provide valuable insights into the relationship between mitochondrial gene expression, and anthracycline intercalation sites.

To examine potential direct effects on mitochondrial DNA integrity and transcription we studied proteins involved in mitochondrial DNA maintenance and transcription. To this end, we made U2OS cell lines in which either mitochondrial transcription factor A (TFAM), factor B2 (TFB2M) or mitochondrial RNA polymerase (mtRNAP) were endogenously tagged with GFP. TFAM coats the mitochondrial genome and, together with TFB2M and mtRNAP, forms the transcription machinery.[17] Microscopic images show that the GFP signal overlaps with the MitoTracker signal, indicating that these proteins localize in the mitochondria (Figure 5).

Protein levels of TFAM were reduced in response to *N,N*-dimethyldoxorubicin, *N,N*-dimethyldaunorubicin and aclarubicin compared to doxorubicin, daunorubicin and the controls etoposide and H_2O_2. Similarly, treatment with the DNA intercalator ethidium bromide, also leads to a significant reduction of TFAM levels. The protein levels of TFB2M and mtRNAP, which act in a complex with TFAM, show a similar trend but to a lesser degree. The rapid degradation of TFAM when not bound to mtDNA, in contrast to stable levels of unbound TFB2M and mtRNAP, may partially explain these results. Through intercalation into mtDNA these anthracyclines may interfere and compete for binding sites of TFAM, hereby instigating TFAM degradation and inhibiting mtDNA transcription. Whether direct protein interactions between anthracyclines and the mitochondrial transcription machinery drive changes in mitochondrial gene expression remains to be elucidated, perhaps through novel immunoprecipitation techniques. Altogether, the preliminary data we obtained regarding the effects of different anthracycline variants on mitochondrial DNA integrity, transcription and translation do not yet provide a conclusive structure-activity relationship study. While all anthracyclines influenced mitochondrial function, the differences between variants were minimal. These results strengthen our hypothesis that cardiotoxicity may primarily arise from DNA damage activity in combination with chromatin damage, as observed with doxorubicin but not with *N,N*-dimethyldoxorubicin.

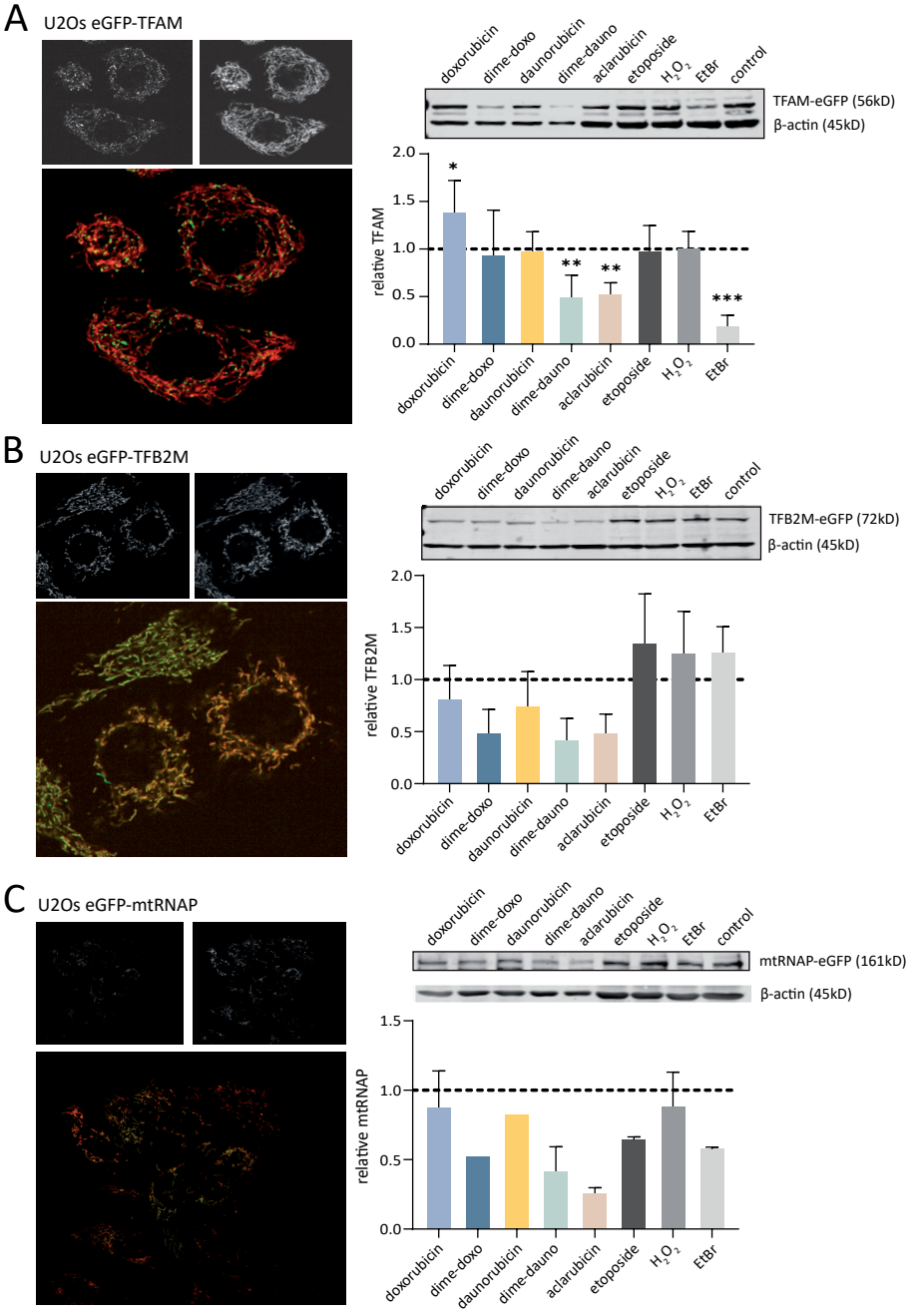

Figure 5 – Protein levels of TFAM, TFB2M and mtRNAP after anthracycline treatment. (A-C) Microscopic validation of endogenously GFP-tagged (A) TFAM, (B) TFB2M and (C) mtRNAP. Mitochondria are labeled with MitoTracker. TFAM, TFB2M and mtRNAP protein levels were quantified with western blot analysis. Ordinary one-way ANOVA with Dunnett's multiple comparison test, * $p < 0,05$; ** $p < 0,01$; *** $p < 0.001$.

The molecular mechanisms through which anthracyclines can inhibit Topo II and induce DNA double strand breaks are well established. In contrast, the discovery that not all anthracyclines cause DNA damage, and that some variants can additionally induce histone eviction is relatively recent. The exact mechanisms by which chromatin damage leads to cell death remain unclear. Therefore, we examined the unique properties of aclarubicin, an anthracycline that does not induce DNA double-strand breaks but does evict histones, leading to chromatin damage. In **chapter 3**, through genome-wide CRISPR-Cas9 knockout screening, we identified p53 as an important regulator of cell death in response to aclarubicin.

Aclarubicin activates a p53-dependent transcriptional program that induces apoptosis, like traditional DNA-damaging anthracyclines, but in the absence of DNA lesions. Aclarubicin-induced chromatin damage resulted in relocalization and activation of p53, and subsequently in p53-dependent apoptosis. Whether p53 itself senses unpacked DNA could not be confirmed in this study. We did however observe relocalization of p53 from the cytoplasm to the nucleus, and more specifically, enhanced binding to chromatin, suggesting that p53 may be part of a DNA sensing complex in response to histone eviction.

Potential interaction partners can be speculated upon based on molecular mechanisms involved in cell death in response to another class of chromatin damaging agents: curaxins. Nucleosome collapse induced by curaxins is sensed by the histone chaperone FACT (Facilitates Chromatin Transcription), which is normally involved in maintaining nucleosome stability during replication, transcription, and DNA repair.[19] Curaxins, which are DNA intercalating agents, can trap the FACT complex on DNA, leading to CK2 activation and subsequent activation of p53.[20] Previous studies have shown that aclarubicin also induces FACT binding to DNA[21], indicating that p53 activation by aclarubicin might be mediated through FACT and CK2. However, this matter is complicated by our finding that p53 is activated through phosphorylation on different serine residues, and it is therefore likely that multiple molecular pathways are involved. The presence of multiple molecular pathways involved in sensing aclarubicin induced chromatin damage may explain why we did not identify any proteins related to the FACT pathway in our screen. This is also consistent with the observation that specific apoptosis inhibitors could not rescue aclarubicin-induced cell death. While the p53-dependent apoptosis pathway may be dominant, tumor cells may also die through alternative pathways in response to aclarubicin.

Overall, this study underscores the critical role of p53 in mediating the cytotoxic effects of aclarubicin and its implications for cancer treatment strategies. Our data demonstrates that cellular sensitivity to aclarubicin can be predicted based on p53 status in *vitro*,

indicating that assessing p53 mutation status could serve as a valuable stratification method to identify patients who would benefit from aclarubicin treatment. Additionally, our results show that aclarubicin synergizes with the BCL-2 inhibitor venetoclax, which has recently been approved for the treatment of chronic lymphocytic leukemia (CLL) and acute myeloid leukemia (AML).[22] Patients could benefit from combination therapy with limited toxicities due to the low adverse effects of both drugs.

Our screen identified p53 as a major determinant of cellular sensitivity to aclarubicin, an anthracycline that primarily causes chromatin damage. However, it is still unknown which factors are involved in the process of histone eviction and the sensing of chromatin damage. To further explore the structure-activity relationship of the molecular characteristics that may dictate histone eviction and chromatin damage, we studied various structurally closely related doxorubicin variants. We included anthracyclines that induce both DNA damage and histone eviction (doxorubicin), those that cause only DNA damage (azido-doxorubicin, hydroxy-doxorubicin, desamino-doxorubicin), and one that only induces histone eviction (*N,N*-dimethyldoxorubicin) (Figure 6).

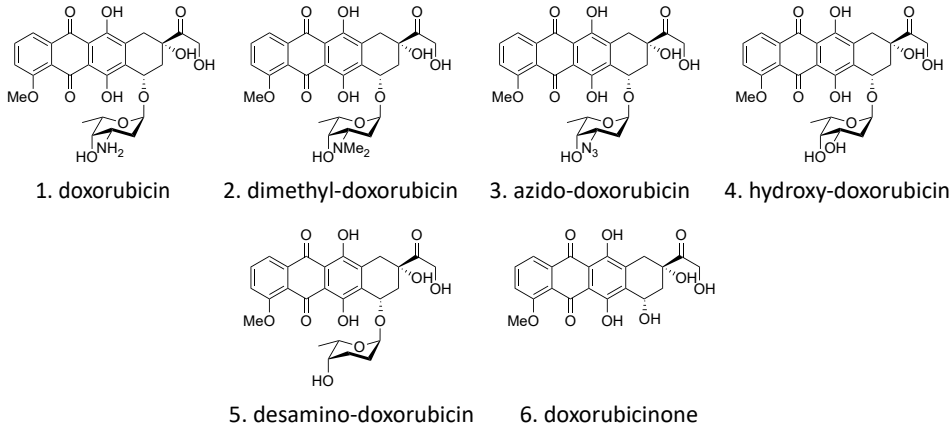

Figure 6 – Chemical structures of doxorubicin analogues.

Cells utilize various ATP-dependent nucleosome remodeling complexes to move, eject or incorporate histones, thereby guiding nucleosome assembly.[23] To determine whether anthracycline-induced histone eviction and nucleosome collapse is mediated by active processes in the nucleus, we compared histone eviction in untreated cells to that in ATP-depleted cells. We showed that histone eviction is not mediated by ATP-dependent processes, but rather occurs as an event that is probably associated with DNA intercalation and competition for space. Doxorubicin and *N,N*-dimethyldoxorubicin induced histone eviction when cells are fully depleted of ATP (Figure S1), whereas azido-doxorubicin,

hydroxy-doxorubicin, desamino-doxorubicin and doxorubinone failed to induce histone eviction altogether independent of ATP levels in the cell (Figure 7).

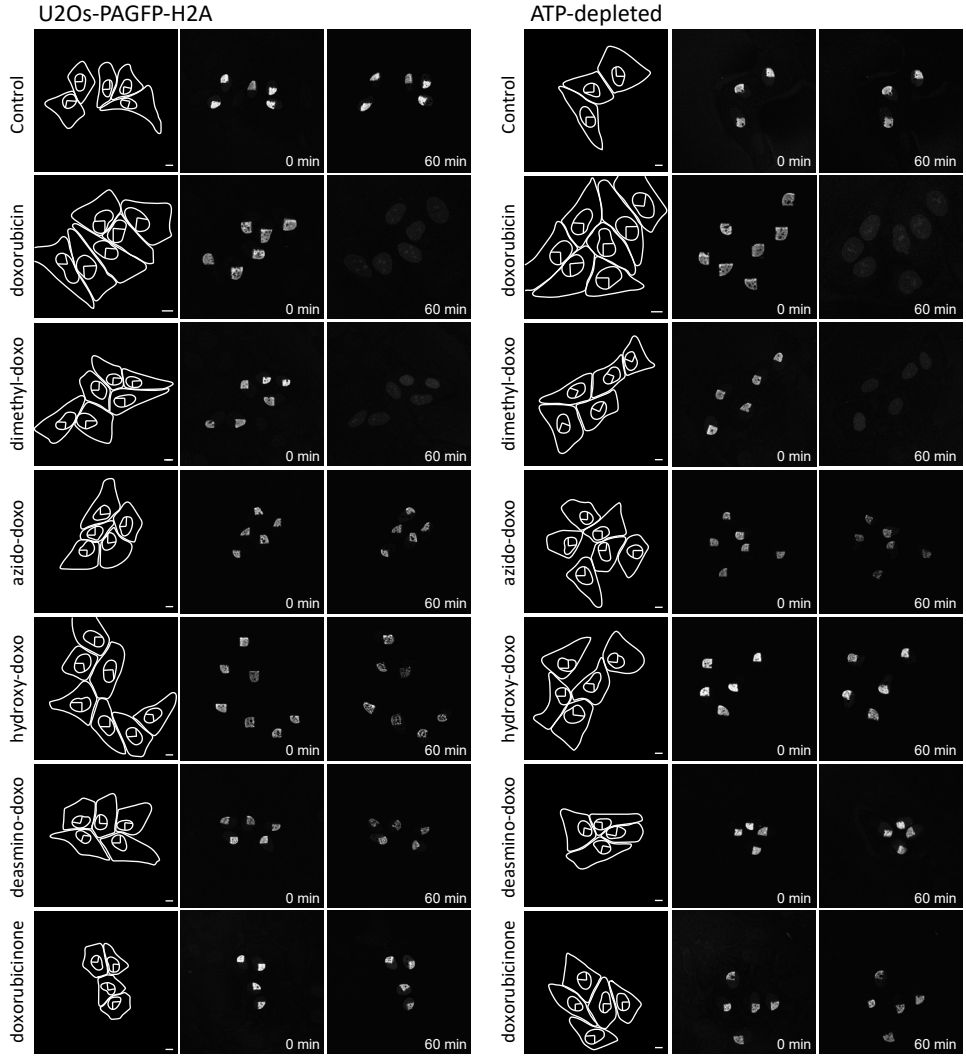

Figure 7 – Histone eviction in response to different doxorubicin analogues. Histone eviction was imaged in living U2Os-PAGFP-H2B cells and ATP-depleted cells. Left panel: cell outline and nucleus, the photoactivated part of the nucleus is indicated. Middle panel shows the photoactivated histones at the onset of the experiment after compound addition. Photo-activation was monitored by time-lapse confocal microscopy for 1 hour in the presence of the indicated compounds at 10 μM. Stills made at 60 min are shown in the right panel. Scale bar, 10 μm.

To study in detail if the intercalation and competition for space with histones is determined by structural differences, we first assessed DNA binding of these anthracyclines in a cell free setup. Here, we compared the properties of different anthracyclines in their displacement of an DNA intercalating dye (Picogreen, Figure 8A) and the displacement of a DNA minor groove binding dye (DAPI, Figure 8B).

All anthracycline variants tested intercalate into double stranded DNA and displace the Picogreen dye, albeit with different affinities. Doxorubicin displays the highest affinity for DNA intercalation in this set, and doxorubicinone the lowest. From crystal structure solution studies on the doxorubicin-DNA complex it was deduced that doxorubicin intercalates into the DNA with the sugar moiety pointing into the minor groove.[24] We performed a dye displacement assay with a minor groove binding dye, and here *N,N*-dimethyldoxorubicin showed the largest dye displacement. Remarkably, doxorubicinone, lacking the sugar moiety, displaces the minor groove binding dye DAPI like the other compounds. This could mean that the minor groove binding dye may dissociate from the DNA because of the intercalating properties that all anthracyclines used here show.

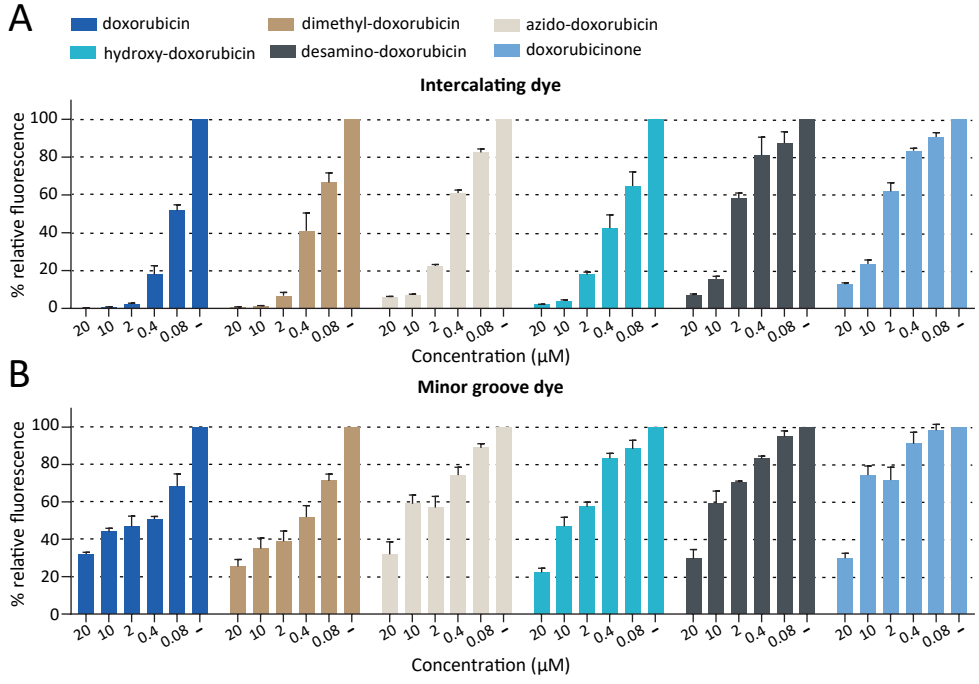

Figure 8 – DNA intercalation affinity of doxorubicin analogues. (A) The intercalation of anthracyclines was tested in a competition dye displacement assay with PicoGreen. The percentage of initial fluorescence is plotted against the concentrations of the indicated compounds. (B) The binding affinity of anthracyclines was measured with the minor-groove binding dye DAPI. The percentage of initial fluorescence is plotted against the concentrations of the indicated compounds.

In addition, we determined nucleosome collapse in cell free conditions in response to different anthracyclines. Reconstituted nucleosomes composed of the histones H2A, H2B, H3 and H4 were incubated with different concentrations of doxorubicin (Figure 9A). There is a clear dose-response relationship for doxorubicin in the disruption of nucleosomes. We compared different anthracycline variants in their capacity to cause histone dissociation, but only doxorubicin and *N,N*-dimethyldoxorubicin cause significant nucleosome collapse (Figure 9B) which is in line with the results published in **chapter 2**. Collectively, the results indicate that histone eviction is not just competition for space between anthracyclines and histones but is more likely determined by many intricate interactions. Since all doxorubicin variants intercalate into the DNA, the sugar-moiety may be a determining factor in the disruption of chromatin structures. The capacity of anthracyclines to induce histone eviction and nucleosome collapse is presumably determined by their structure, and independent of active processes within the cellular environment.

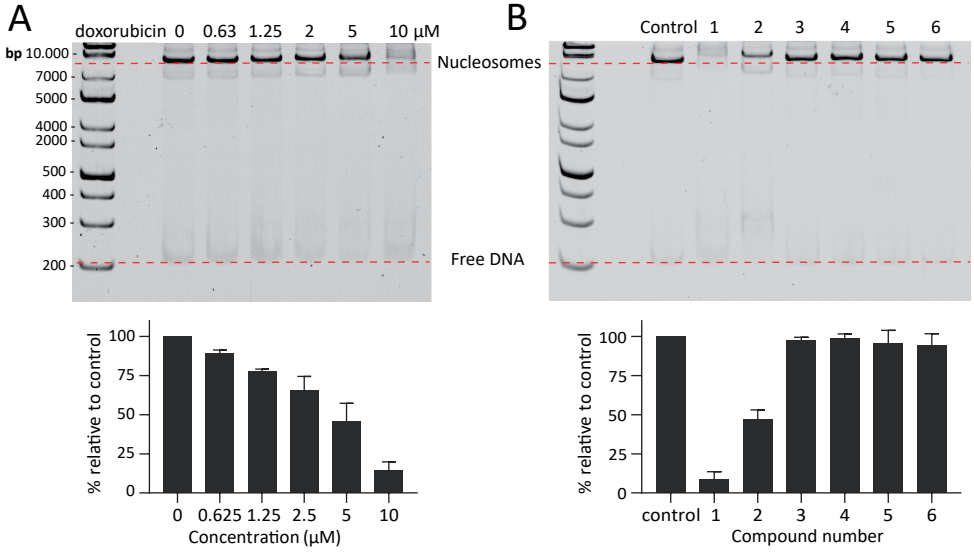

Figure 9 – Reconstituted nucleosome integrity in the presence of doxorubicin analogues. (A) Nucleosomes were incubated with different concentrations of doxorubicin. Results are quantified relative to untreated control. (B) Nucleosomes were incubated with different doxorubicin analogues at a concentration of 10µM. Results are quantified relative to untreated control. Incubation with doxorubicin or *N,N*-dimethyldoxorubicin induces nucleosome collapse.

Ultimately, higher resolution techniques are essential to study DNA intercalation and nucleosome collapse in more detail. Magnetic tweezers measurements could shed more light on the nanomechanical properties of DNA winding and unwinding in the presence

of anthracyclines. Such studies have been performed in the past for doxorubicin and daunorubicin[25,26], but larger structure-activity relationship studies with the different doxorubicin variants could greatly enhance our understanding. Recently, a very elegant method was reported to label nucleosomal DNA for nuclear magnetic resonance (NMR) spectroscopy studies. In this study, it was observed that aclarubicin binds the exposed AT-rich minor groove and, and that it is likely that the drug invades nucleosomes from the terminal ends inward, eventually resulting in histone eviction.[27] This method opens new opportunities to study the structural dynamics of nucleosomal DNA, and it may be possible to compare different anthracycline variants.

Resistance to anthracyclines presents a significant hurdle in cancer treatment and is often mediated by ATP-binding cassette (ABC) transporters that actively pump compounds across the plasma membrane, diminishing their efficacy. We previously demonstrated that the combination of DNA damage and histone eviction exerted by doxorubicin drives its associated adverse effects. However, whether the same properties dictate drug resistance is unclear.

In **chapter 4**, we evaluated a library of 40 anthracyclines on their cytotoxicity in cancer cell lines overexpressing the ABCB1 transporter or ABCG2 transporter. We identified several highly cytotoxic anthracyclines, that stand out due to their effectiveness in doxorubicin-resistant cells. We identified structural variants of the clinically used anthracyclines doxorubicin, epirubicin, daunorubicin, idarubicin and aclarubicin that outperform their respective partner compounds. We performed more in-depth analyses with these compounds, to identify how structural variations affect intracellular uptake, subcellular localization, DNA intercalation and Topo II inhibition in ABCB1-overexpressing, doxorubicin-resistant cells. Two of these anthracycline variants warrant further investigation: *N,N*-dimethyl-idarubicin and a related idarubicin variant composed of the idarubicin aglycon and the aclarubicin trisaccharide stand out, due to their histone eviction-mediated cytotoxicity toward doxorubicin-resistant cells.

This study focuses on the limitations of anthracyclines in clinical use — doxorubicin, daunorubicin, epirubicin and idarubicin — due to treatment-related toxicities and drug resistance. Previously we showed that doxorubicin and its analogues exert their anticancer effects through two independent mechanisms: inducing DNA double-strand breaks and causing chromatin damage via histone eviction. Notably, *N,N*-dimethyldoxorubicin, a compound that only induces histone eviction, showed reduced side effects compared to its clinical counterparts. We assessed a total of 40 anthracycline variants, of which their molecular mechanisms were determined in **chapter 2**, for their cytotoxicity in doxorubicin-resistant cells overexpressing ABCB1 or ABCG2. We showed that all anthracyclines that are currently in clinical use are less effective against ABCB1-

overexpressing cells, confirming their status as ABCB1 substrates. In contrast, a total of 16 of the novel anthracycline variants retained their cytotoxicity in drug- resistant cells, demonstrating potential for overcoming ABCB1 and ABCG2-mediated drug resistance. Anthracyclines featuring *N,N*-dimethyl amino sugars were shown to be less likely substrates for ABCB1, enhancing their therapeutic potential. This study highlights several promising structural variants, most notably *N,N*-dimethyl-idarubicin and *N,N*-dimethyl-idarubicin trisaccharide. The cytotoxicity of these anthracyclines is not compromised by the overexpression of drug transporters, and due to their histone-eviction mediated cytotoxic they may be less damaging than their traditional counterparts. These compounds not only bypass common resistance mechanisms but also exhibit enhanced nuclear accumulation, which correlates strongly with their efficacy.

Overall, we gained valuable insights into the design of new, safer anthracycline drugs and showed that specific structural modifications can enhance their effectiveness in drug resistant cells. Further exploration of the most promising compounds in preclinical studies is warranted. Future research should first confirm the anti-tumor efficacy of proposed *N,N*-dimethyl-idarubicin analogues in *in vivo* models. If their potency is as good as expected based on the *in vitro* results, it is of utmost importance to research if these compounds are also less cytotoxic to healthy cells and therefore may cause less side effects.

In conclusion, while anthracyclines remain cornerstone treatments in oncology due to their effectiveness, it is essential to address their associated toxicities and resistance mechanisms. Ongoing research should focus on minimizing adverse effects and improving the therapeutic use to enhance treatment outcomes and patients' quality of life.

Methods

Reagents and antibodies

Doxorubicin was obtained from Accord Healthcare Limited, UK, daunorubicin was obtained from Sanofi, aclarubicin (sc-200160) and doxorubicinone (sc-218273) were purchased from Santa Cruz Biotechnology (USA), etoposide was obtained from Pharmachemie (the Netherlands). *N,N*-dimethyl-doxorubicin, *N,N*-dimethyl daunorubicin, azido-doxorubicin, hydroxy-doxorubicin and desamino-doxorubicin were synthesized as described previously.[28]

Cell culture

AT-3 cells (provided by R. Arens, LUMC, The Netherlands), U2OS cells (ATCC, HTB-96) and H9c2 cells (provided by M. Goumans, LUMC, The Netherlands) were maintained in DMEM medium supplemented with 8% FCS. All cell lines were maintained in a humidified atmosphere of 5% CO_2 at 37 °C, regularly tested for the absence of mycoplasma and the origin of cell lines was validated using short tandem repeat (STR) analysis.

U2OS cells were endogenously GFP-tagged for TFAM, TFB2M and mtRNAP, as described previously. In short, gRNA sequences for each target protein were designed using the publicly available CRISPOR tool and subsequently cloned into the pX330/Cas9 vector. Making use of homologous recombination constructs with flanking HDRs as on the pX330 vector, both plasmids were used to co-transfect U2OS cells. Cells were single-cell FACS sorted and validated using confocal microscopy and western blot.

Flow cytometry

Cells were treated with 10 μM compound for 2 hours. Samples were washed with PBS, collected, and fixed with paraformaldehyde. Samples were analyzed by flow cytometry using BD FACS Aria II, with 561-nm laser and 610/20-nm detector. The cellular uptake of anthracyclines was quantified using FlowJo software.

Constant-Field Gel Electrophoresis (CFGE)

Cells were seeded into 12-well format (200.000 cells/well), treated with 5 μM of each compound or 200 μM of H_2O_2 for 2 hours. Subsequently, drugs were removed by extensive washing and cells were collected and processed immediately. DNA double strand breaks were quantified by constant-field gel electrophoresis as described.[29]

Long-range PCR for mitochondrial DNA damage

Cells were seeded in a 12-well plate (100.000 cells/well) and treated with 5 μM of the indicated compounds, or 100 μM H_2O_2 for 2 hours. Cells were subsequently washed and total DNA was isolated using the Isolate II Genomic DNA kit (Meridian Bioscience). Quantitative long-range PCR method was performed as described previously[30], to measure mitochondrial DNA damage. Primers used were described before, supplied by Integrated DNA Technologies: FW small (5'-CCCAGCTACTACCATCATTCAGT-3'); RV small (5'-GATGGTTTGGGAGATTGGTTGATGT-3'); FW large (5'-GCCAGCCTGACCCATAGCCATAATAT-3'); RV large (5'-GAGAGATTTTATGGGTGTAATGCGG-3'). PCR-fragments were run on agarose gels, stained with ethidium bromide, imaged using the Molecular Imager Gel Doc XR system (Bio-Rad). Images were analyzed using ImageStudio (v5.2) and relative amplification was quantified and normalized to controls.

DNA intercalation competition assay

Plasmid DNA of 17.8kb (100ng) was incubated with a concentration range indicated compounds to a final volume of 10 µL and incubated for 5 min at RT. Samples were run on a 0.8% agarose gel for 25 min on 100 V and subsequently stained using 0,5 µg/mL EtBr for 30 min followed by de-staining in ultra-pure water for 15 min. Gels were imaged with the Molecular Imager Gel Doc XR system (Bio-Rad).

RT-qPCR

U2OS or H9c2 cells were treated with 5 µM of each anthracycline or 100 µM H_2O_2 and 0,5 µg/mL EtBr for 2 hours. Subsequently, cells were washed and RNA was isolated 4 hour post treatment using the ISOLATE II RNA mini kit (Meridian Bioscience). For cDNA synthesis Transcriptor High Fidelity cDNA synthesis kit (Roche Life Science) was used. qPCR was performed with the SensiFAST SYBR No-ROX kit (Meridian Bioscience) and measured using the Bio-Rad CFX384 imager. Primers were designed and described before[31–34]. For analysis, Ct values were normalized against the expression of *GAPDH* and relative expression against the untreated control was quantified with the $2^{-\Delta\Delta CT}$ method.

Gene	Cell line	Primer Sequences
GAPDH	H9c2	FW: *CTCGTCTCATAGACAAGATGGT*
		RV: *GGGTAGAGTCATACTGGAACATG*
	U2OS	FW: *TACTAGCGGTTTTACGGGCG*
		RV: *TCGAACAGGAGGAGCAGAGAGCGA*
mt-ND1	H9c2	FW: *TCCTCCTAATAAGCGGCTCCTTCT*
		RV: *TGGTCCTGCGGCGTATTCG*
	U2OS	FW: *CCACCTCTAGCCTAGCCGTTTA*
		RV: *GGGTCATGATGGCAGGAGTAAT*
mt-CYB	H9c2	FW: *TACGCTATTCTACGCTCCATTC*
		RV: *GCCTCCGATTCATGTTAAGACTA*
	U2OS	FW: *ATCACTCGAGACGTAAATTATGGCT*
		RV: *TGAACTAGGTCTGTCCCAATGTATG*
mt-CO1	H9c2	FW: *GCCAGTATTAGCAGCAGGTATCA*
		RV: *GCCGAAGAATCAGAATAGGTGTTG*
	U2OS	FW: *GACGTAGACACACGAGCATATTTCA*
		RV: *AGGACATAGTGGAAGTGAGCTACAAC*

Western Blot

Cells were seeded (200.000 cells/well) and treated with 5 µM of each compound or 200 µM of H_2O_2 for 2 hours. For western blot, cells were washed with PBS and lysed in SDS-sample buffer (2%SDS, 10% glycerol, 5% β-mercaptoethanol, 60 mM Tris-HCl pH 6.8, and

0.01% bromophenol blue). Samples were separated by SDS-PAGE and transferred to a nitrocellulose membrane. Blocking of the filters and antibody incubations were done in PBS supplemented with 0.1% (v/v) Tween and 5% (w/v) milk powder (skim milk powder, LP0031, Oxiod). Blots were imaged by an Odyssey Classic imager (Li-Cor).

Histone eviction

For PAGFP-H2A photoactivation and time-lapse confocal imaging, U2OS-PAGFP-H2A cells were seeded in a 35 mm glass bottom petri dish (Poly-d-lysine-Coated, MatTek Corporation). Cells were treated with 10μM of the indicated compounds for 1 hour. For ATP-depletion cells were pre-incubated for 30 minutes with 0.01% NaAz and 10mM 2-deoxyglucose. Time-lapse confocal imaging was performed on a Leica SP8 confocal microscope system 63x lens, equipped with a climate chamber as described previously.

DNA Dye Competition Assay

1 μg/mL circular double-stranded DNA was incubated with Quant-iT PicoGreen dsDNA reagent (Thermo Fisher Scientific, P7581) or DAPI (Thermo Fisher Scientific, D1306) for 5 min at RT. Subsequently, indicated drug concentrations were added to the DNA/dye mixture and incubated for another 5 min at RT followed by measurement of fluorescence using a CLARIOstar plate reader (BMG Labtech) excitation 480 nm / emission 520 nm (480-20/520-10 filter) Picogreen, excitation 350nm / emission 465 nm (350-20/465-10 filter). Fluorescence was quantified relative to that of the untreated controls. Fluorescent signals of all samples were corrected for the corresponding drug concentrations in the absence of DNA.

Nucleosome assembly and collapse

Mono nucleosomes were assembled from recombinant human histones expressed in *E. coli* (two each of histones H2A, H2B, H3 and H4. Accession numbers: H2A-P04908; H2B-O60814; H3.1-P68431; H4-P62805) wrapped by provided 217 base pair DNA sequence that includes the Widom 601 sequence with an added GATC (EpiCypher, 16-1410). Mono nucleosomes were incubated with indicated compounds for 5 minutes at RT. Nucleosomes were subsequently resolved on a 8% native poly-acrylamide gel and stained with ethidium bromide. Gels were imaged with the Molecular Imager Gel Doc XR system (Bio-Rad).

References

(1) Brockmann, H. Anthracyclinones and Anthracyclines. (Rhodomycinone, Pyrromycinone and Their Glycosides). *Fortschritte der Chemie organischer Naturstoffe,* **1963,** *21*, *121-182*.

(2) van der Zanden, S. Y.; Qiao, X.; Neefjes, J. New Insights into the Activities and Toxicities of the Old Anticancer Drug Doxorubicin. *FEBS Journal*. **2021**, *288*, 6095–6111.

(3) Mattioli, R.; Ilari, A.; Colotti, B.; Mosca, L.; Fazi, F.; Colotti, G. Doxorubicin and Other Anthracyclines in Cancers: Activity, Chemoresistance and Its Overcoming. *Molecular Aspects of Medicine*. **2023**, *93*, 101205.

(4) Qiao, X.; Van Der Zanden, S. Y.; Wander, D. P. A.; Borràs, D. M.; Song, J. Y.; Li, X.; Duikeren, S. Van; Gils, N. Van; Rutten, A.; Herwaarden, T. Van; Tellingen, O. Van; Giacomelli, E.; Bellin, M.; Orlova, V.; Tertoolen, L. G. J.; Gerhardt, S.; Akkermans, J. J.; Bakker, J. M.; Zuur, C. L.; Pang, B.; Smits, A. M.; Mummery, C. L.; Smit, L.; Arens, R.; Li, J.; Overkleeft, H. S.; Neefj, J. Uncoupling DNA Damage from Chromatin Damage to Detoxify Doxorubicin. *Proceedings of the National Academy of Sciences of the United States of America*. **2020**, *117*, 15182–15192.

(5) Mortensen, S. A. Aclarubicin: Preclinical and Clinical Data Suggesting Less Chronic Cardiotoxicity Compared with Conventional Anthracyclines. *European Journal of Haematology*. **1987**, *38*, 21–31.

(6) Rothig, H. J.; Kraemer, H. P.; Sedlacek, H. H. Aclarubicin: Experimental and Clinical Experience. *Drugs under experimental and clinical research*. **1985**, *11*, 123–125.

(7) Huang, K. M.; Hu, S.; Sparreboom, A. Drug Transporters and Anthracycline-Induced Cardiotoxicity. *Pharmacogenomics*. **2018**, *19*, 883–888.

(8) Yakes, F. M.; Van Houten, B. Mitochondrial DNA Damage Is More Extensive and Persists Longer than Nuclear DNA Damage in Human Cells Following Oxidative Stress. *Proceedings of the National Academy of Sciences of the United States of America*. **1997**, *94*, 514–519.

(9) Abe, K.; Ikeda, M.; Ide, T.; Tadokoro, T.; Miyamoto, H. D.; Furusawa, S.; Tsutsui, Y.; Miyake, R.; Ishimaru, K.; Watanabe, M.; Matsushima, S.; Koumura, T.; Yamada, K. I.; Imai, H.; Tsutsui, H. Doxorubicin Causes Ferroptosis and Cardiotoxicity by Intercalating into Mitochondrial DNA and Disrupting Alas1-Dependent Heme Synthesis. *Science Signaling*. **2022**, *15*.

(10) Yin, J.; Guo, J.; Zhang, Q.; Cui, L.; Zhang, L.; Zhang, T.; Zhao, J.; Li, J.; Middleton, A.; Carmichael, P. L.; Peng, S. Doxorubicin-Induced Mitophagy and Mitochondrial Damage Is Associated with Dysregulation of the PINK1/Parkin Pathway. *Toxicology in Vitro*. **2018**, *51*, 1–10.

(11) Termini, J. Hydroperoxide-Induced DNA Damage and Mutations. *Mutation research*. **2000**, *450*, 107–124.

(12) Santos, J. H.; Meyer, J. N.; Mandavilli, B. S.; Van Houten, B. Quantitative PCR-Based Measurement of Nuclear and Mitochondrial DNA Damage and Repair in Mammalian Cells. *Methods in molecular biology (Clifton, N.J.)*. **2006**, *314*, 183–199.

(13) Yang, F.; Kemp, C. J.; Henikoff, S. Anthracyclines Induce Double-Strand DNA Breaks at Active Gene Promoters. *Mutation research*. **2015**, *773*, 9.

(14) Anderson, S.; Bankier, A. T.; Barrell, B. G.; De Bruijn, M. H. L.; Coulson, A. R.; Drouin, J.; Eperon, I. C.; Nierlich, D. P.; Roe, B. A.; Sanger, F.; Schreier, P. H.; Smith, A. J. H.; Staden, R.; Young, I. G. Sequence and Organization of the Human Mitochondrial Genome. *Nature*. **1981**, *290*, 457–465.

(15) Wu, B. Bin; Leung, K. T.; Poon, E. N. Y. Mitochondrial-Targeted Therapy for Doxorubicin-Induced Cardiotoxicity. *International Journal of Molecular Sciences*. **2022**, *23*, 1912.

(16) Pang, B.; de Jong, J.; Qiao, X.; Wessels, L. F. A.; Neefjes, J. Chemical Profiling of the Genome with Anti-Cancer Drugs Defines Target Specificities. *Nature chemical biology*. **2015**, *11*, 472–480.
(17) Taanman, J. W. The Mitochondrial Genome: Structure, Transcription, Translation and Replication. *Biochimica et biophysica acta*. **1999**, *1410*, 103–123.
(18) Chaires, J. B.; Fox, K. R.; Herrera, J. E.; Britt, M.; Waring, M. J. Site and Sequence Specificity of the Daunomycin-DNA Interaction. *Biochemistry*. **1987**, *26*, 8227–8236.
(19) Neefjes, J.; Gurova, K.; Sarthy, J.; Szabó, G.; Henikoff, S. Chromatin as an Old and New Anti-Cancer Target. *Trends in cancer*. **2024**, *10*, 696.
(20) Gasparian, A. V.; Burkhart, C. A.; Purmal, A. A.; Brodsky, L.; Pal, M.; Saranadasa, M.; Bosykh, D. A.; Commane, M.; Guryanova, O. A.; Pal, S.; Safina, A.; Sviridov, S.; Koman, I. E.; Veith, J.; Komar, A. A.; Gudkov, A. V.; Gurova, K. V. Curaxins: Anticancer Compounds That Simultaneously Suppress NF-KB and Activate P53 by Targeting FACT. *Science Translational Medicine*. **2011**, *3*.
(21) Nesher, E.; Safina, A.; Aljahdali, I.; Portwood, S.; Wang, E. S.; Koman, I.; Wang, J.; Gurova, K. V. Role of Chromatin Damage and Chromatin Trapping of FACT in Mediating the Anticancer Cytotoxicity of DNA-Binding Small-Molecule Drugs. *Cancer research*. **2018**, *78*, 1431–1443.
(22) Juárez-Salcedo, L. M.; Desai, V.; Dalia, S. Venetoclax: Evidence to Date and Clinical Potential. *Drugs in Context*. **2019**, *8*, 212574.
(23) Clapier, C. R.; Iwasa, J.; Cairns, B. R.; Peterson, C. L. Mechanisms of Action and Regulation of ATP-Dependent Chromatin-Remodelling Complexes. *Nature reviews. Molecular cell biology*. **2017**, *18*, 407.
(24) Frederick, C. A.; Williams, L. D.; Ughetto, G.; van der Marel, G. A.; van Boom, H. J.; Rich, A.; Wang, A. H. J. Structural Comparison of Anticancer Drug-DNA Complexes: Adriamycin and Daunomycin. *Biochemistry*. **1990**, *29*, 2538–2549.
(25) Liu, T.; Cai, T.; Huo, J.; Liu, H.; Li, A.; Yin, M.; Mei, Y.; Zhou, Y.; Fan, S.; Lu, Y.; Wan, L.; You, H.; Cai, X. Force-Enhanced Sensitive and Specific Detection of DNA-Intercalative Agents Directly from Microorganisms at Single-Molecule Level. *Nucleic Acids Research*. **2024**, *52*, e86–e86.
(26) Salerno, D.; Brogioli, D.; Cassina, V.; Turchi, D.; Beretta, G. L.; Seruggia, D.; Ziano, R.; Zunino, F.; Mantegazza, F. Magnetic Tweezers Measurements of the Nanomechanical Properties of DNA in the Presence of Drugs. *Nucleic Acids Research*. **2010**, *38*, 7089.
(27) van Emmerik, C. L.; Lobbia, V.; Neefjes, J.; Nelissen, F. H. T.; van Ingen, H. Monitoring Anthracycline Cancer Drug-Nucleosome Interaction by NMR Using a Specific Isotope Labeling Approach for Nucleosomal DNA. *ChemBioChem*. **2024**, *25*, e202400111.
(28) van Gelder, M. A.; van der Zanden, S. Y.; Vriends, M. B. L.; Wagensveld, R. A.; van der Marel, G. A.; Codée, J. D. C.; Overkleeft, H. S.; Wander, D. P. A.; Neefjes, J. J. C. Re-Exploring the Anthracycline Chemical Space for Better Anti-Cancer Compounds. *Journal of Medicinal Chemistry*. **2023**, *66*, 11390–11398.
(29) Wlodek, D.; Banáth, J.; Olive, P. L. Comparison between Pulsed-Field and Constant-Field Gel Electrophoresis for Measurement of DNA Double-Strand Breaks in Irradiated Chinese Hamster Ovary Cells. *International journal of radiation biology*. **1991**, *60*, 779–790.
(30) Furda, A. M.; Bess, A. S.; Meyer, J. N.; Van Houten, B. Analysis of DNA Damage and Repair in Nuclear and Mitochondrial DNA of Animal Cells Using Quantitative PCR. *Methods in molecular biology (Clifton, N.J.)*. **2012**, *920*, 111.
(31) Lei, Y.; Vanportfliet, J. J.; Chen, Y.-F.; Upton, J. W.; Li, P.; Phillip, A.; Correspondence, W.; Bryant, J. D.; Li, Y.; Fails, D.; Torres-Odio, S.; Ragan, K. B.; Deng, J.; Mohan, A.; Wang, B.; Brahms, O. N.; Yates, S. D.; Spencer, M.; Tong, C. W.; Bosenberg, M. W.; West, L. C.; Shadel, G. S.; Shutt, T. E.; West, A. P.

Cooperative Sensing of Mitochondrial DNA by ZBP1 and CGAS Promotes Cardiotoxicity. *Cell*. **2023**, *186*, 3013-3032.e22.

(32) Ferreira, A.; Cunha-Oliveira, T.; Simões, R. F.; Carvalho, F. S.; Burgeiro, A.; Nordgren, K.; Wallace, K. B.; Oliveira, P. J. Altered Mitochondrial Epigenetics Associated with Subchronic Doxorubicin Cardiotoxicity. *Toxicology*. **2017**, *390*, 63–73.

(33) Guan, G.; Yang, L.; Huang, W.; Zhang, J.; Zhang, P.; Yu, H.; Liu, S.; Gu, X. Mechanism of Interactions between Endoplasmic Reticulum Stress and Autophagy in Hypoxia/Reoxygenation-Induced Injury of H9c2 Cardiomyocytes. *Molecular Medicine Reports*. **2019**, *20*, 350.

(34) Wallace, L. S.; Mehrabi, S.; Bacanamwo, M.; Yao, X.; Aikhionbare, F. O. Expression of Mitochondrial Genes MT-ND1, MT-ND6, MT-CYB, MT-COI, MT-ATP6, and 12S/MT-RNR1 in Colorectal Adenopolyps. *Tumour biology : the journal of the International Society for Oncodevelopmental Biology and Medicine*. **2016**, *37*, 12465.

Supporting Information chapter 5

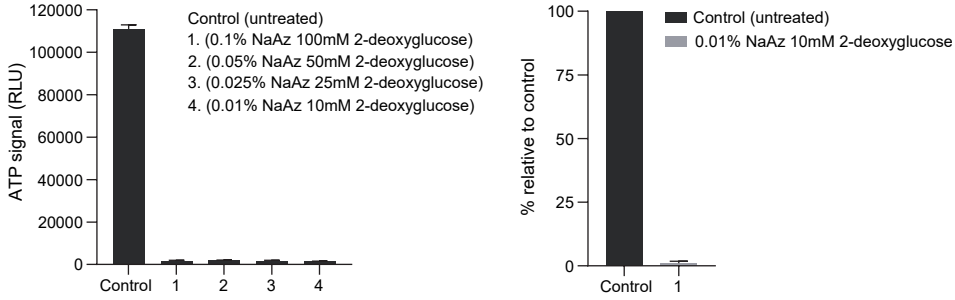

Figure S1 – ATP depletion validation for different conditions in U2OS cells. Total ATP levels were measured in U2OS cells in response to different concentrations of sodium azide and 2-deoxyglucose.

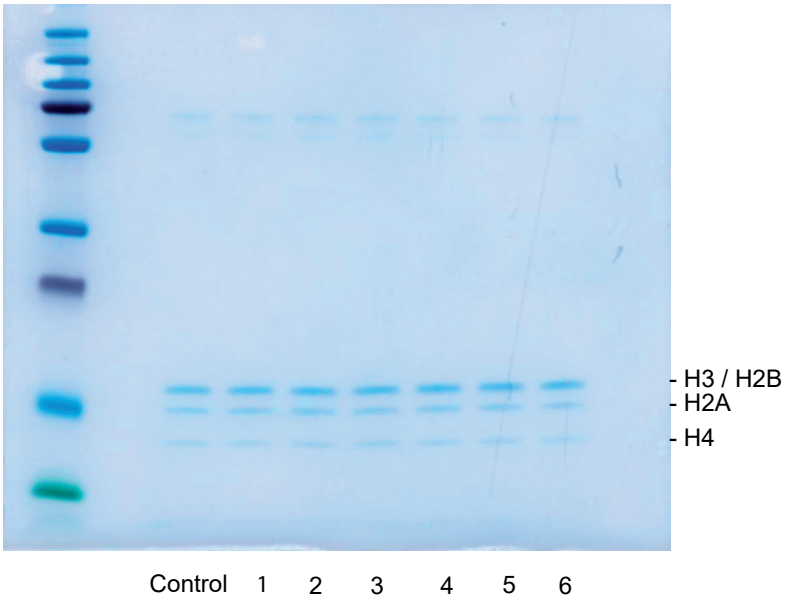

Figure S2 – Coomassie staining of mono nucleosomes. Total protein levels are shown for all treatments compared to untreated control.